RELATIONSHIP BETWEEN CYCLIC UNDRAINED TRIAXIAL STRENGTH OF SANDY SOIL AND GEOTECHNICAL INDEX VALUES

Koichiro YOKOTA and Tsuneo IMAI

Abstract

(Objectives)

The methods for finding and comparing earthquake induced shear stress and cyclic undrained shear strength of the ground are well known. These values are used to evaluate the liquefaction potential of the ground. Of the various methods available for determining these values, those considered to be the most accurate are the earthquake ground response analysis method for earthquake induced shear stress, and the cyclic undrained triaxial test, conducted in the laboratory to determine cyclic undrained shear strength of the ground.
The objective of this paper is to present the process by which the authors have worked out an experimental formula that is very useful in the evaluation of cyclic undrained triaxial strength (hereafter referred to as Rl_{20}) on the basis of other geotechnical index values. The authors' new formula is the product of data derived from numerous cyclic undrained triaxial tests.
The formula was worked out by applying the following multiple regression analysis method:

$$Rl_{20}=\beta_0+\Sigma\beta_i X_i$$

where β_0=intercept, β_i=multiple regression coefficient, X_i=geotechnical index values.

(Summary)

An axial loading type cyclic triaxial apparatus was used for the experiments. Figures 1 and 2 show a schematic view of the apparatus and a detailed diagram of the cell respectively. Undisturbed samples for use in the experiment were taken from alluvial sandy deposits and sandy reclaimed ground layers by means of sand sampling. All samples were frozen immediately after collection. Table 1 is the list of the whole samples used for cyclic triaxial testing.

Figure 3 shows some typical wave form records produced in the experiments. Basically the records taken in the experiments were of 3 types: cyclic axial loading, cylic axial displacement and excess pore water pressure.

Figure 4 is a graphic definition of Rl_{20}. It defines Rl_{20} as the stress ratio (stress ratio is the ratio of 1/2 the single amplitude of cyclic axial stress and initial effective confining pressure) obtained when a sinusoidal axial wave is applied to the sample 20 times, making axial double amplitude of displacement equivalent to 5 % strain.

At first, the authors considered effective overburden pressure $\sigma v'$, dry density γ_d, relative density Dr, mean diameter D_{50}, 10% diameter D_{10}, fine content FC and N-value(which is defined as the number of blow counts in the standard penetration test) as possible geotechnical index values that could be used to indicate Rl_{20}. However, because of problems in obtaining and evaluating data, it was finally decided to use only $\sigma v'$, N-value, D_{50} and FC.

Altogether, 142 samples were taken. At each given depth, 1 sample (divided into 3 or 4 specimens) was takan.

Figures 5 through 12 show the relationships between Rl_{20} and various geotechnical index values. None of these graphs show good correlations. This led the authors to consider multiple regression analysis.

Figure 13 shows the correlation coefficients between the variables used in multiple regression analysis. It will be noted that a fairly close correlation exists between D_{50} and FC, which seems to be perfectly natural. These two variables were not considered together in the multiple regression formula. Table 2. based on the above determinations, shows all possible combinations of multiple regression analysis. The multiple regression formula for Rl_{20} was solved for all these combinations. For $\log Rl_{20}$, the formula was solved only for three combinations that should show statistical significance. (See Fig. 14 ①—③ and Fig. 15)

Both Rl_{20} computation results in Figure 14 and $\log Rl_{20}$ computation results in Figure 15 are shown as multiple correlation coefficients and variance ratios in the two graphs.

Of these computation results, it was found that the multiple correlation coefficient whose value is highest results from combinations of $\log Rl_{20}$, $\log \sigma v'$, N and $\log FC$. This is shown by the following experimental formula.

$$\log Rl_{20} = -0.785 + N \cdot \log 1.012 + 0.0868 \log FC - 0.441 \log \sigma v'$$

In other words

$$Rl_{20} = 0.164 \cdot (1.012)^{N} \cdot (FC)^{0.0868} \cdot \sigma v'^{-0.441} \cdots\cdots \text{(See formula (3) of thesis)}$$

Figure 16 shows the relationship between the final values for Rl_{20} as obtained by the formula (3) (calculated Rl_{20}) and those Rl_{20} values actually measured (measured Rl_{20}). The graph also shows the relationship using existing data. The correlations can be said to be good.

Figure 17 shows the same information as Figure 16, using data obtained from the existing formula. (See formula (5) of thesis). No general pattern can be discerned in this graph. Then main difference between the formula (3) and the formula (5) lies in the nature of the dependency of both formulas on N-value and $\sigma v'$.

Most research to date has found cyclic undrained shear strength to be greatly affected by N-value in clean sand. In this aspect, the formula (5) is in good agreement with the traditional view of the N-value and cyclic undrained shear strength relationship. However, the formula (3) can be considered superior than the formula (5) for determining cyclic undrined shear strength by sand sampling and cyclic triaxial testing. From another point of view, the formula (3) can be considered to cast doubt on the relative accuracy of the presently used systems for evaluating cyclic undrained shear strength. This area should be considered to be a subject for further study.

1 INTRODUCTION

In recent years, liquefaction of sandy ground during earthquakes has come to the fore as an important field of research. Research includes the nature of this type of ground and the design of structures to be built on it. Many methods have been proposed for predicting ground liquefaction. The methods range from quite simple ones, using only two properties such as soil grain characteristics and N-value and conducting computer analysis to quite complex methods. The most accurate method to date for evaluating liquefaction potential is to compares earthquake induced shear stress of the ground and cyclic undrained shear strength. The most common methods used to determine shear stress are the wave propagation theory, the lumped mass method, the finite element method, etc. These techniques are used to conduct analysis of ground response during earthquakes. For analysis of shear strength of the ground,

the most commonly used methods are cyclic triaxial testing and cyclic simple shear testing.

The object of this paper is to present the derivation of an experimental formula showing the relationship between cyclic undrained triaxial strength and four geotechnical index values, that is, N-value, mean diameter, fine content and effective overburden pressure. The actual formula was developed using multiple regression analysis. Until the present, many attempts have been made to discover the relationship between cyclic undrained triaxial strength and soil properties. All of these attempts have explored the apparent relationship between two or three variables, objectively combining these tendencies to produce a certain formula. The authors have attempted here to evaluate as objectively as possible the relationship between each variable to produce a suitable experimental formula.

2 TESTING APPARATUS

Figure 1 shows in outline the testing apparatus used. The specimen is placed within the cell, in which a certain confining pressure is maintained. A certain number of cyclic loads are applied in the direction of the axis, and the relationship between the number of loads applied and displacement, pore water pressure, etc, are recorded. While cofining pressure is applied by means of a compressor, cyclic pressure is applied in the form of oil pressure. A semi-conductor type pressure transducer detects static pressure (confining pressure) by electric

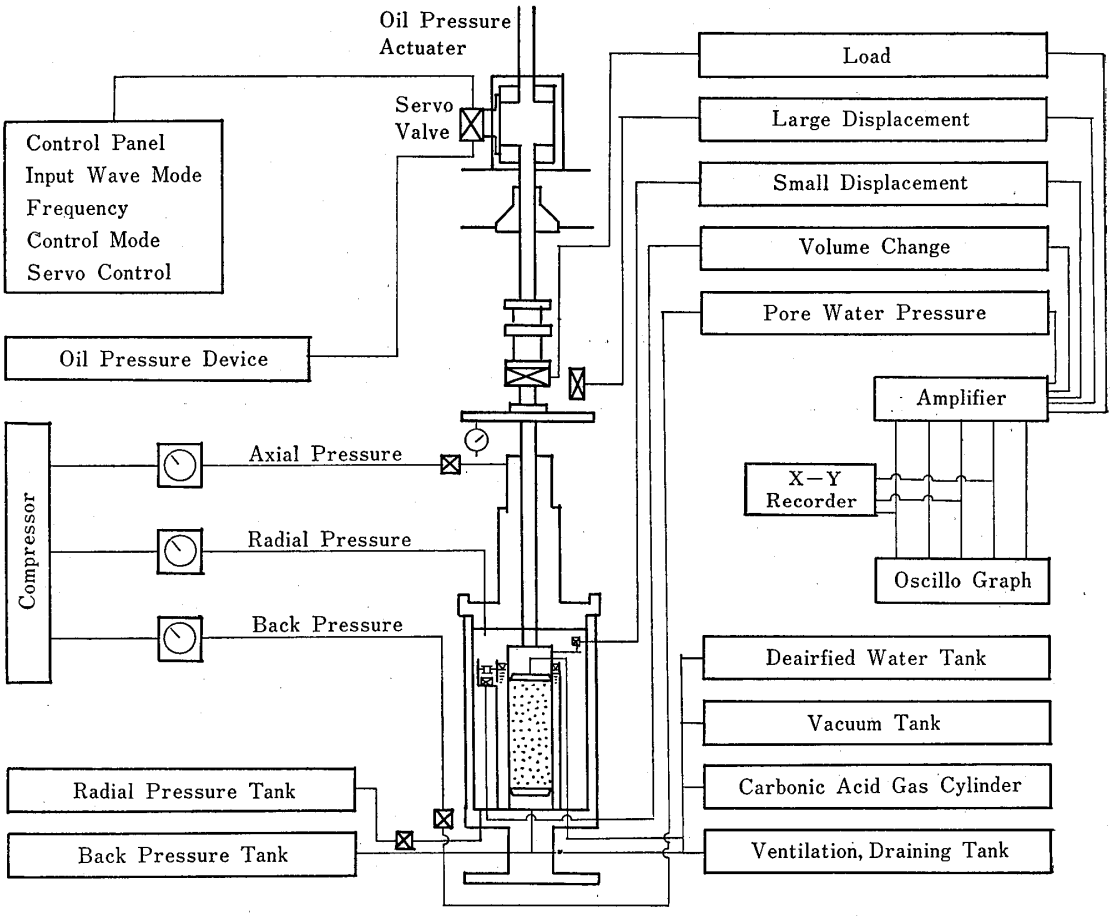

Fig. 1 Schematic view f the apparatus

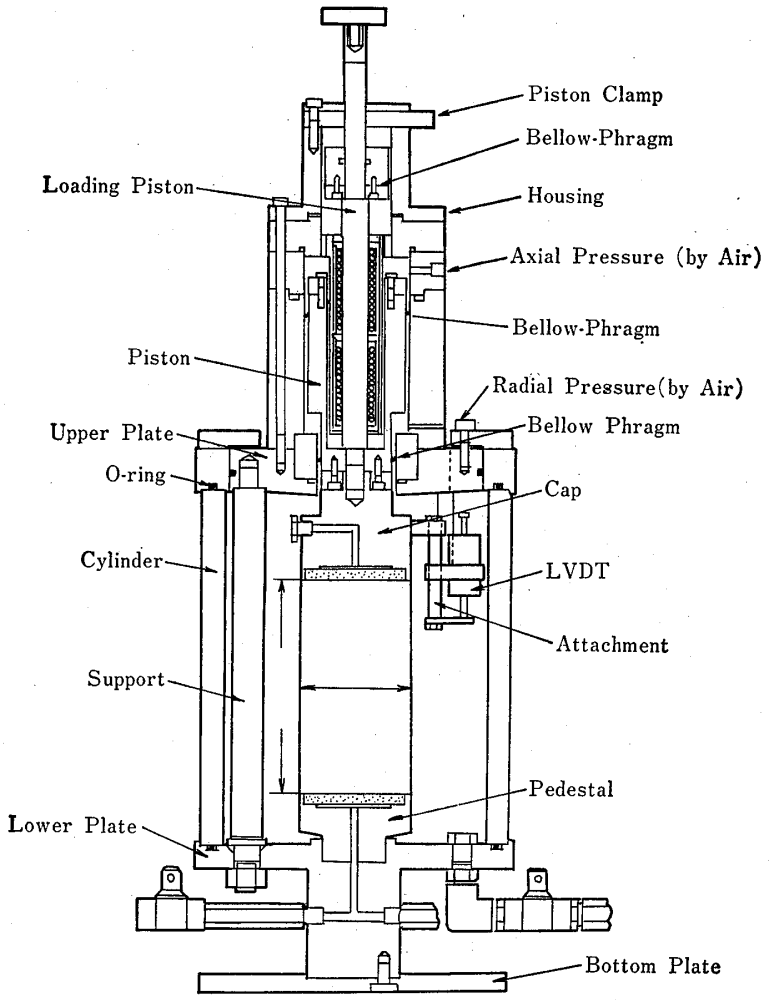

Fig. 2 Detail of the cell

measuring. Cyclic load is measured with the load cell. Two LVDTs measure displacement. Pore water pressure is measured by the same type of transducer used in static pressure measurement.

Various kinds of cyclic wave forms are possible for testing, including sine waves, rectangular waves and certain random input waves.

The following information is necessary to obtain accurate experimental results:

static pressure	8 km/cm^2 max
cyclic loading	±250kg max
frequency	0.1 to 5 Hz

The lower right hand section of Figure 1 is a carbonic acid gas circulation system. This system is used for quickly and completely saturating sandy soil specimens.

Next, let us explain the detailed diagram of the cell in Figure 2. The cell uses 3 bellowphragms to seal the piston section. The piston is centered by means of bearings in the central section. This type of structure permits independent control of axial and lateral pressure. Thus, subsoil stress conditions can be recreated at will. This is the outstanding feature of the cell. In other ways, it is almost the same as the ordinary triaxial cell.

3 SAMPLES USED IN TESTING

All samples used in testing consisted of sandy soil from alluvial deposits or reclaimed land areas. All undisturbed samples were obtained by twist sampler.[1] Fine content of all samples taken amounted to as much as 60%. Table 1 summarizes the types of samples used in testing. All saturated samples taken from below ground level were frozen at the site and stored in a freezer at the laboratory. Afterwards, these samples were removed from the freezer and reduced to specimens of either 50mm diameter and 100mm length or 70mm diameter and 140mm length with the aid of a saw, file, etc. It should be noted that the diameter of the samples are predetermined by the diameter of the twist samplers, so that the main objective in cutting the specimens was to establish uniform lengths.

Table 1 Samples used for cyclic triaxial testing

Site	Major soil type	Remarks	
A (Aichi Pref.)	fine to med. sand	reclaimed sand alluvial sand *N*-value	(Dep.$<$ 5 m) (Dep.$\geqq$ 5 m) 5~25
B (Chiba Pref.)	silty to fine sand	reclaimed sand alluvial sand *N*-value	(Dep.$<$10m) (Dep.$\geqq$10m) 5~25
C (Kagawa Pref.)	med. to coarse sand	reclaimed sand alluvial sand *N*-value	(Dep.$<$ 5 m) (Dep.$\geqq$ 5 m) 5~15
D (Saitama Pref.)	silty to fine sand	alluvial sand *N*-value	(Dep.$<$ 6 m) 5~15
E (Chiba Pref.)	silty to fine sand	reclaimed sand alluvial sand *N*-value	(Dep.$<$ 6 m) (Dep.$\geqq$ 6 m) 5~20
F (Miyagi Pref.)	med. to gravelly sand	alluvial sand *N*-value	 10~40
G (Miyagi Pref.)	med. to gravelly sand	alluvial sand *N*-value	 5~20

4 TESTING PROCEDURE

(1) *Setting of Specimen in Triaxial Cell*

After trimming the specimen, diameter, length, weight, etc. are measured carefully, and the specimen is covered with a rubber membrane and set in the triaxial cell. It is important that this part of the operation be carried out quickly, before the specimen thaws.

(2) *Thawing of the specimen*

Next, the specimen is thawed by subjecting it to a 0.2kg/cm^2 vacuum for 2 hours.

(3) *Saturation of the Sample*

Samples in general arrive at the laboratory in a somewhat unsaturated condition. As it is important that the liquefaction test be conducted on a completely saturated specimen, this is accomplished by circulating carbonic acid gas and deaerafied water in turns through the specimen, and applying an appropriate back pressure load to attain complete satuation. Since carbonic acid gas is 100 times more water-soluble than air, this process of saturation is highly efficient. Saturation is confirmed by using Skempton's pore pressure coefficient. This coefficient is defined as follows:

$$\beta=\frac{\Delta U}{\Delta\sigma} \tag{1}$$

where

$\Delta\sigma$=increase of confining pressure, and

ΔU=increase of pore water pressure in an undraind condition when confining pressure $\Delta\sigma$ increases. When $\beta=1.00$ the specimen is completely saturated.

In the tests conducted by the authors, β was equal to or exceeded 0.95 for all specimens.

(4) *Consolidation of the Specimen*

When saturation was complete, the specimens were consolidated at isotropic confining pressure that was equivalent to effective overburden pressure. Consolidation time was set at about 2 hours. Back pressure was applied during consolidation.

(5) *Cyclic Undrained Shear Test*

When consolidation is complete, a sine wave cyclic load is applied in the direction of the axis, with a cyclic load frequency of 0.5 Hz or 1.0 Hz. Cyclic loading, displacement and pore water pressure are automatically recorded. The test is continued until double axial strain amplitude exceeds 10%.

5 INTERPRETATION OF TEST RESULTS AND DEFINITION OF CYCLIC UNDRAINED TRIAXIAL STRENGTH

Figure 3 shows representative examples of recordings taken during testing. The purpose of the liquefaction test is to investigate the way that increases in displacement and excess pore water pressure occurs in response to cyclic pressure at a fixed amplitude. Cycic loading, displacement and changes in pore water pressure are recorded, and cyclic undrained triaxial strength is calculated. Cyclic undrained triaxial strength tells us the relationship between stress ratio (the ratio of 1/2 the single amplitude of cyclic axial atress and initial effective confining pressure) and the number of cyclic loadings necessary for liquefaction to occur (the authors refer to this number as *Nl*). Stress ratio is easily determined on the basis of cyclic load, sectional area of the specimen and effective confining stress. There are various methods for detemining *Nl*. Here, *Nl* is defined as the necessary number of cyclic loadings for double ampliude of axial strain to reach 5%.[2] In this way, stress ratio and *Nl* can be determined for each specimen.

As a rule, 3 or 4 specimens were taken at each given depth, so that 3 or 4 sets of data for each depth was made available. Figure 4 shows that cyclic undrained triaxial strength is most commonly defined as the stress ratio value that yields a 5% strain obtained on the application of the 20th cyclic load.[3] This paper uses the same definition (see Figure 4). In order to plot a smooth curve, it is, of course, necessary to provide a sufficient spread between

Nl-values. In general, *Nl* frequencies should be obtained with sufficient spread between values, within a range of 100 cycles. Cyclic undrained triaxial strength as determined according to this definition will henceforth be referred to as Rl_{20}.

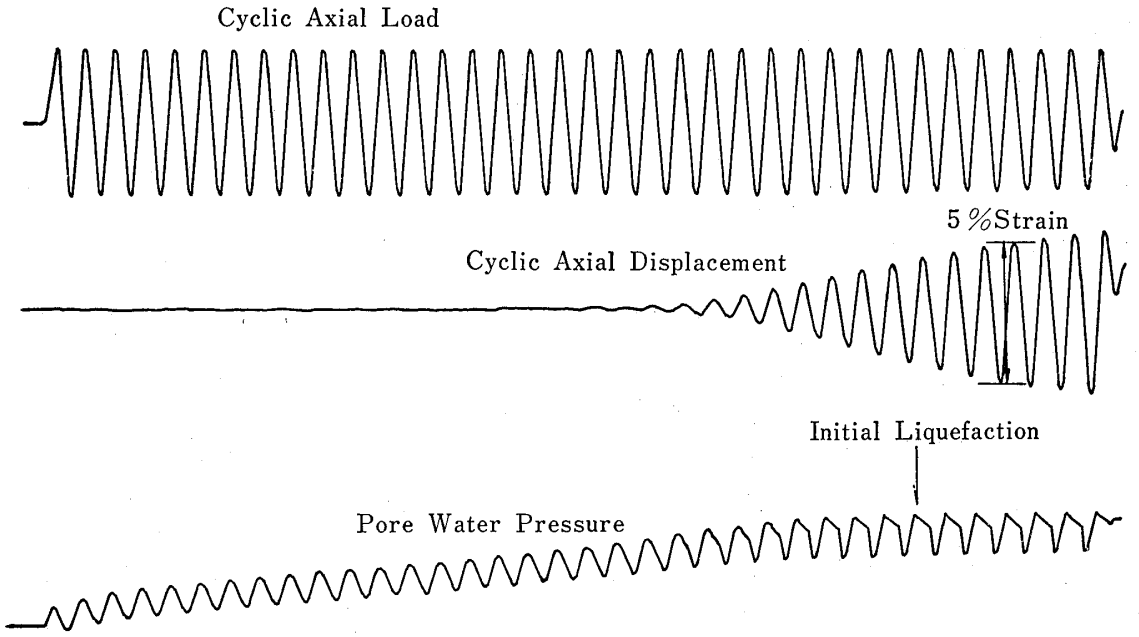

Fig. 3 Typical record of wave form

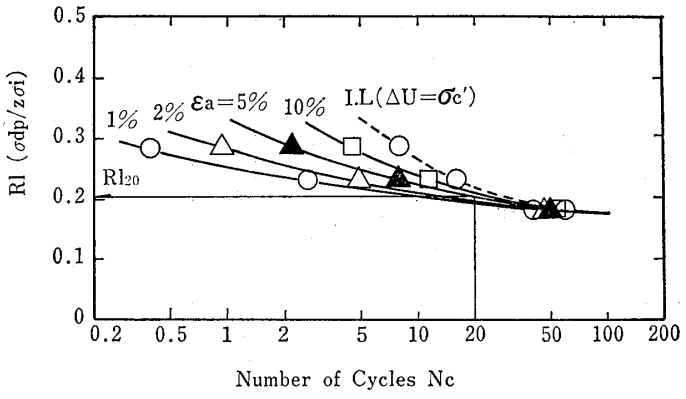

Fig. 4 Definition of Rl_{20}

6 GENERAL RELATIONSHIP OF TEST RESULTS TO GEOTECHNICAL INDEX VALUES

What soil characteristics can be found to show a basic relationship with cycic undrained triaxial strength Rl_{20}? In pursuit of such relationships, the authors first considered the following geotechnical index value of soil:

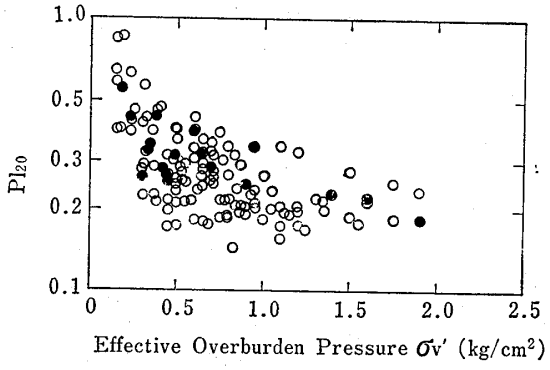

Fig. 5 Relationship between Rl_{20} and $\sigma v'$

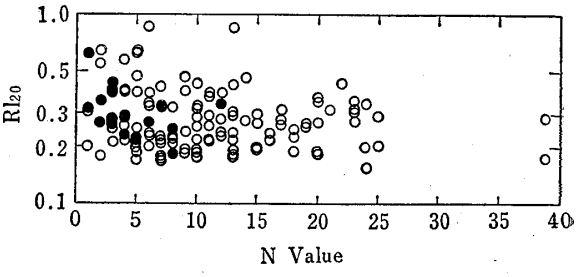

Fig. 6 Relationship between Rl_{20} and N-value

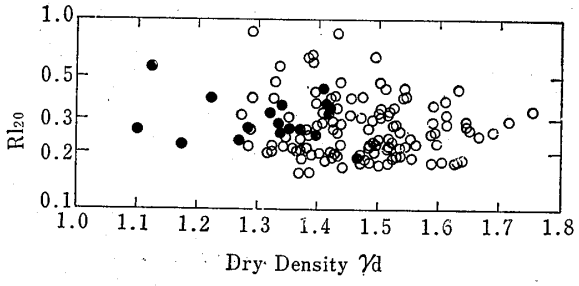

Fig. 7 Relationship between Rl_{20} and γ_d

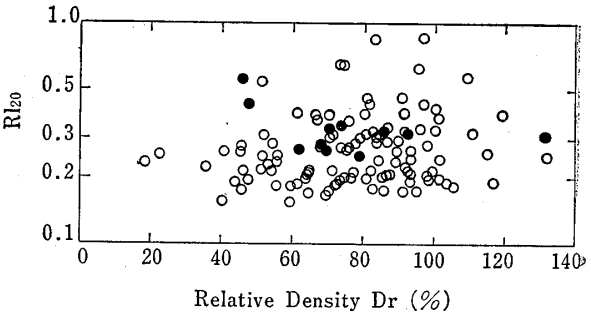

Fig. 8 Relationship between Rl_{20} and Dr

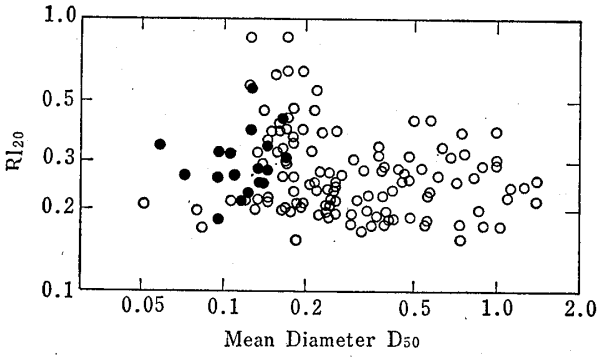

Fig. 9 Relationship between Rl_{20} and D_{50}

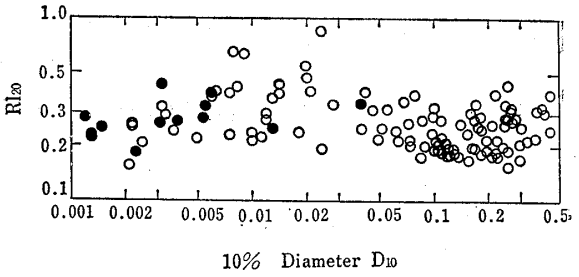

Fig.10 Relationship between Rl_{20} and D_{10}

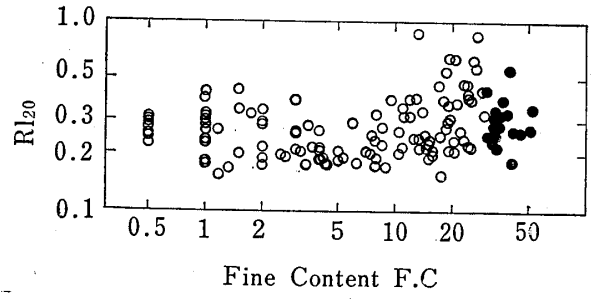

Fig.11 Relationship between Rl_{20} and FC

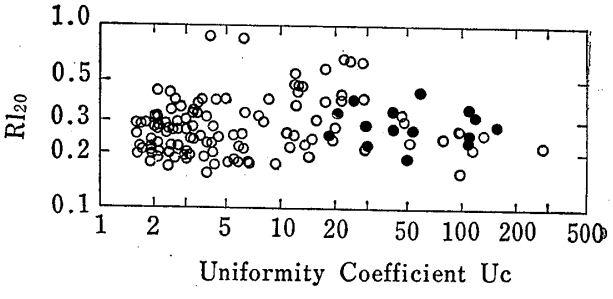

Fig.12 Relationship between Rl_{20} and Uc

$\sigma v'$=in situ effective overburden pressure
N-value=number of blow counts in the standard penetration test
γ_d=dry density of specimen during testing
Dr=relative density of specimen during testing
D_{50}=mean diameter
D_{10}=diameter of grain corresponding to 10% of grain-size accumulation curve
FC=fine content
Uc=uniformity coefficient

Figures 5 through 12 show the relationships between Rl_{20} and these constants. The black circles in these graphs represent samples in which $30\% \leqq FC \leqq 60\%$, while the white circles represent samples in which $FC < 30\%$. These graphs were plotted on the basis of a total of 142 samples (each sample consisting of 3 or 4 specimens). Some Dr values were not measured. Also, some values for D_{10} and Uc were undeterminable.

In each of these graphs, there is a great deal of scatter, so that no clear tendency can be discerned. However, somewhat of a negative correlation between Rl_{20} and $\sigma v'$ can be seen.

Two major reasons can be cited to explain why a greater relationship between Rl_{20} and the various geotechnical index values cannot be discerned. First, although there is generally considered to be a strong relationship between cyclic undrained triaxial strength and such structural characteristics of soil as configuration, shape and orientation of grain, no index values that adequately express these characteristics exist.[4] Such techniques as microphotography, x-rays, etc. are frequently used to investigate these characteristics, but these techniques cannot be said to constitute simple soil investigation methods, and were not used in the present research.

We must conclude that the above coefficients alone are not enough to completely explain cyclic undrained triaxial strength.

The second factor is that due to the presense of numerous influential factors, merely finding an overt relationship between Rl_{20} and other independent variables does not constitute establishing a good correlation.

This paper considers the above point in its use of multiple regression analysis to extrapolate relationships between these constants to find a suitable experimental formula.

7 DERIVATION OF EXPERIMENTAL FORMULA BY MULTIPLE REGRESSION ANALYSIS

(1) *The Multiple Regression Analysis Method*

This method will be very simply touched on here. If one has a variable, Y whose changes can be thought to be explained by a number of variables, X_i, Y may be expressed by the following formula :

$$Y=\beta_0+\Sigma\beta_i X_i \tag{2}$$

The method of statistically determining the most appropriate values for β_0 and β_i is called multiple regression analysis. In the formula, Y is a dependent variable, X_i represents indepndent variables, β_0 is the intercept, and β_i represents multiple regression coefficients. In this paper, Y is expressed as Rl_{20} and X_i is geotechnical index values. The usefulness of the multiple regression analysis formula may be judged according to the values obtained for multiple correlation coefficients and variance ratio. The significance of the multiple regression coeficient can be judged by comparing T-value with T-value distribution.

(2) *Variables Used in Calculation*

The dependent variable used, of course, was Rl_{20}. As mentioned in section 6, independent variables that could be used include $\sigma v'$, N-value, Dr, D_{50}, D_{10}, FC, Uc, etc. However, using all these variables would have only resulted in complicating calculations to no particular advantage. Thus, the independent variables used were limited according to the following specifications:

* Values which could not be obtained by simple methods were eliminated.
* Values which sometimes cannot be determined according to their own definition were eliminated.

Strictly speaking. $\sigma v'$ cannot be accurately determined without samples being taken in each layer. However, in actual practice, a great deal of sampling is taken in alluvium clayey soil, while in sandy soil, unit weight may be inferred without too great an error, even without sampling. Consequently, if ground water shows hydrostatic pressure distribution, determination of $\sigma v'$ is an easy matter.

N-value is pretty much of an indispensable value in soil exploration, and is also easy to obtain.

Since γ_d and Dr require dry density values of samples, undisturbed sand samling is required to determine these values. Essentially, the object of undisturbed sand sampling is to take samples for cyclic triaxial testing. The cost is high. Thus, it is not approprite to use this method only for determination of dry density. D_{50} can be easily obtained by mechanical analysis. D_{10} can also be simply obtained by mechanical analysis, but there are some cases when the value cannot be detemined. FC can always be determined by mechanical analysis. As with D_{10}, Uc can usually be determined by mechanical analysis, but there are some cases when the value cannot be determined.

On the basis of the above reasoning, the independent variables to be used in multiple regression analysis were limited to N-value, $\sigma v'$, D_{50} and FC. However, when the correlation coefficients between each of the independent variables were obtaind (see Figure 13) it was found that D_{50} and FC show a close relationship in comparison with the other variables. Thus, it was decided not to consider both these values as indispensable variables at the same time. It was also decided to analyze the logarithms of all these values, including Rl_{20}.

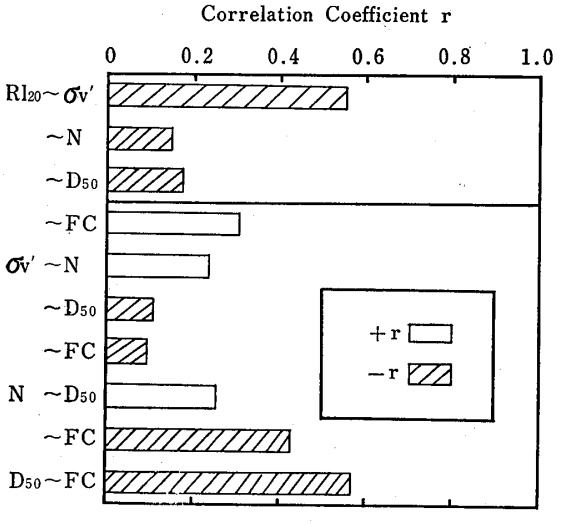

Fig.13 Correlation coefficient between variables

Table 2 Combinations of multiple regression analysis

Dependent variable	Independent variables		
Rl_{20} or log Rl_{20}	$\sigma v'$	N	D_{50} or FC
	log $\sigma v'$	N	D_{50} or FC
	$\sigma v'$	log N	D_{50} or FC
	$\sigma v'$	N	log D_{50} or log FC
	$\sigma v'$	log N	log D_{50} or log FC
	log $\sigma v'$	N	log D_{50} or log FC
	log $\sigma v'$	log N	D_{50} or FC
	log $\sigma v'$	log N	log D_{50} or log FC

Table 2 shows the possible combinations of variables that could be solved for in multiple regression analysis. First, the authors solved for all combinations using Rl_{20}. However, it was decided to solve for only what was considered to be the 3 most suitable combinations using Rl_{20} as a logarithmic expression.

(3) *Calculation Results*

Figure 14 shows the results of calculating the different variables combined with Rl_{20} (as shown in Table 2). The results are multiple correlation coefficients and variance ratios. Those combinations marked with an x represent either one or more multiple regression coefficients whose significance level does not amount to 1%. Those combinations marked with ①, ② and ③ are combinations of relatively high value multiple correlation coefficients that have not been eliminated as having a low significance level. In addition, each variance ratio of ①, ② and ③surpass the F-value calibration 1% level. Multiple regression analysis was carried out for each of these three combinations, with Rl_{20} as a logarithmic expression. Figure 15 shows the results. In addition, calculation was carried out for samples whose fine content was less than or equal to 60% (all samples) and for those whose fine content was less than or equal to 30%. In each case, the multiple correlation coefficient was largest when the independent variables were taken as $\log \sigma v'$, N-value and $\log FC$. Furthermore, the use of Rl_{20} in the form of a logarithmic expression most accurately expresses experimental results.

Thus, the following formula was obtained.

$$Rl_{20}=0.164\cdot(1.012)^{N}\cdot(FC)^{0.0868}\cdot\sigma v'^{-0.441}\quad(FC\leqq 60\%) \tag{3}$$

$$Rl_{20}=0.159\ (1.012)^{N}\cdot(FC)^{0.0967}\cdot\sigma v'^{-0.468}\quad(FC\leqq 30\%) \tag{4}$$

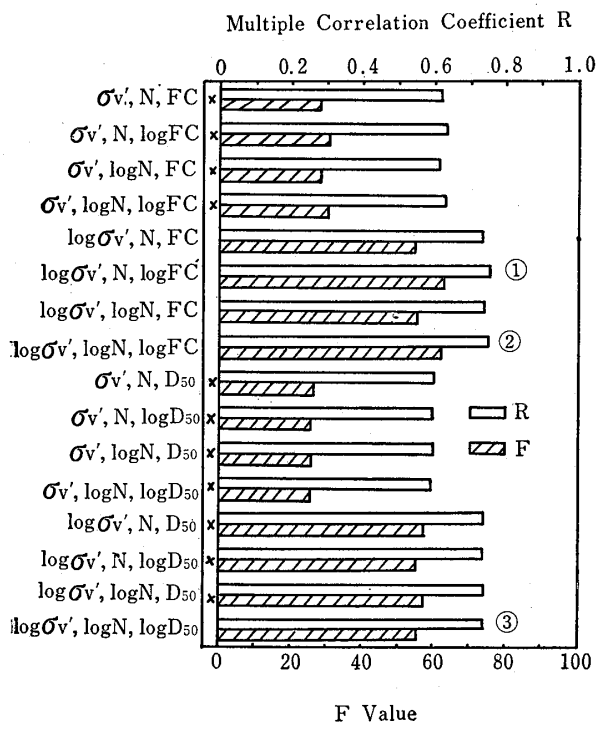

Fig.14 Results of multiple regression analysis

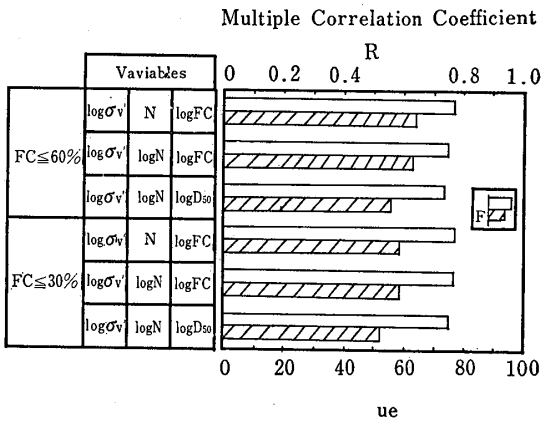

Fig.15 Results of multiple regression analysis

8 DISCUSSION

Figure 16 shows the correspondance between the values calculated for Rl_{20} using Formula (3) and actually measured values. These calculated values were obtained using Formula (3). The graph also shows previously available data results.[5),6),7)]

In figure 16, both ordinate and abcissa are logarithmic expressions. These graphs shows a good deal of scatter, but fairly good correspondence.

The exact range of applicability of the independent variables of Formula (3), as detemined by conditions at time of experimentation are as follows:

$$\sigma v' : 0.15 \leqq \sigma v' \leqq 1.9 \quad \text{kg/cm}^2$$
$$N : 1 \leqq N \leqq 39$$
$$FC : 0.5 \leqq FC \leqq 53 \quad \%$$

Other attempts have been made to establish a connection between geotechnical index values and Rl_{20}. The following formula is representaive of these: [3)]

$$Rl_{20} = 0.0882\sqrt{\frac{N}{\sigma v' + 0.7}} - 0.225 \log\frac{D_{50}}{0.35} \quad (0.04 \leqq D_{50} \leqq 0.6\text{mm})$$
$$Rl_{20} = 0.0882\sqrt{\frac{N}{\sigma v' + 0.7}} - 0.05 \quad (0.6 \leqq D_{50} \leqq 1.5\text{mm}) \qquad (5)$$

Let us consider the meaning of this formula. First, the cyclic undrained shear stress of sand and the relative density of a specimen are said to show the following relationship: [3)]

$$Rl_{20} = 0.0042 \cdot Dr \qquad (6)$$

Using the research results of Gibbs and Holtz, Meyerhef derived the following formulas: [8),9)]

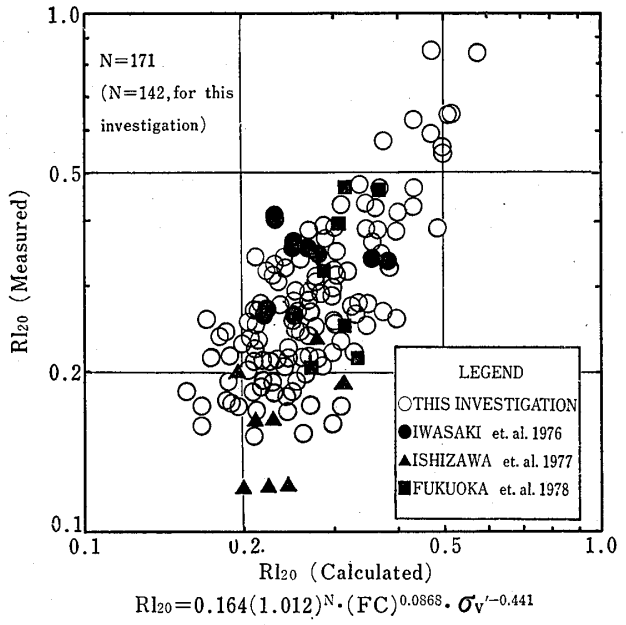

Fig.16 Comparison between Rl_{20}-measured with Rl_{20}-calculated

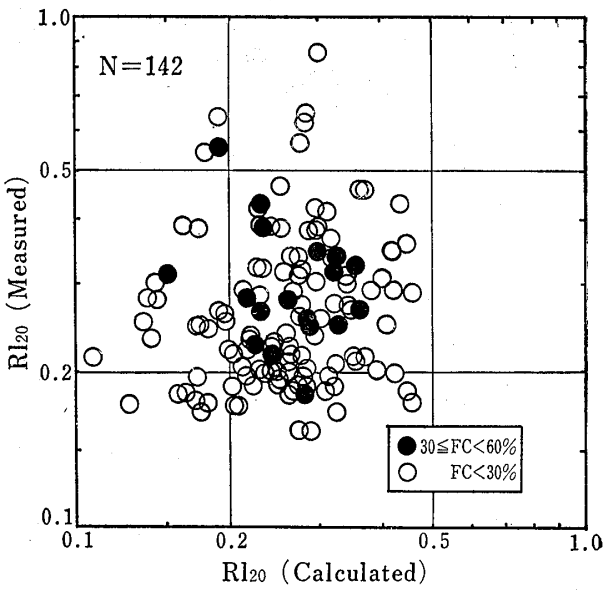

Fig.17 Comparison between Rl_{20}-measured with Rl_{20}-calculated using formula (5)

$$Dr^*=21\sqrt{\frac{N}{\sigma v'+0.7}} \tag{7}$$

Dr^* and Dr do not always shows agreement. However, if we tentatively substitute Dr^* for Dr, Formula (6) changes to the following:

$$Rl_{20}=0.0882\,Dr^* \tag{8}$$

Formula (8) is determined by effective overburden pressure and N-value. It will be noted that N-value is greatly influenced by grain size distribution. Thus a correction term is used, such as the second term on the right side of Formula (5).

Figure 17 shows the correspondance between the actual Rl_{20} value and what it should be according to Formula (5). The graph shows much scattering with no recognizable pattern.

Taking the above into consideration, we may conclude that, as a formula based on a combination of results from sand sampling and cyclic undrained triaxial testing to express cyclic undrained shear strength, Formula (3) is superior to formula (5). However, on the other hand, the dependency of Formula (3) on N-value is relatively small, so that even if N-value changes from 5 to 20, shear strength increases only by a factor of 1.2. This appears to be a small value, and if accurate, shows that N-value has little relationship with ground improvement.

From a completely different point of view, if it is true that cyclic undrained shear strength has a close relationship with N-value, we must begin to doubt the accuracy of the results obtained using the cyclic undrained triaxial testing system with sand sampling. We may consider as one possible reason error in sand sampling. In sand sampling, sand that is dense becomes loose, while loose sand becomes dense. Consequently, the difference as expressed as cyclic undrained triaxial strength is small.[10] Also, the formula reported herein depends greatly within a restricted range on $\sigma v'$. This has to do with error resulting from such factors as friction of the piston within the cell, effects of the rubber membrane and precision of the loadcell and LVDT.

In any case, there is a necessity for continued research to improve sand sampling, laboratory liquefaction testing and the eqipment used therein. In addition, many-faceted research, including use of ground models, aimed at developing methods for evaluating liquefaction strength at the site and exploring the phenomenon of liquefaction are necessary.

REFERENCES

1) T. Imai and K. Yokota, (1978): "Sand Sampling Using Twist Sampler." Sampling symposium. Japanese Soc. Soil Mech. Found. Eng. p. 109—114. (In Japanese)
2) K. Ishihara, M. Sodekawa, U. Tanaka. (1978): "Effects of Overconsolidation On Liquefaction Characteristcs of Fine Content Sand." Dynamic Geotechnical Testing, ASTM STP 654. p. 246—264.
3) F. Tatsuoka, I. Iwasaki, K. Tokida, S. Yasuda, M. Hirose, T. Imai, M. Konno, (1978): "A Method For Estimating Undrained Cyclic Strength of Sandy Soils Using Standard Penetration Resistance." Soils and Foundations, Vol. 18. No. 3, p. 43—58.
4) J. P. Mulilis, H. B. Seed, C. K. Chan, J. K. Mitchell, K. Arulanandan. (1977): "Effects of Sample Preparation on Sand Liquefaction." Journal of the Geotechnical Engineering division. ASCE Vol. 103, GT 2, p. 91—108.
5) Technical Memorandum of the Public Works Research Institute, (1976): "Aseismic Soil Exploration of Akebonobashi and Shintatsumibashi Area of Tokyo Wangan Road." (In Japanese)

5) M. Ishizawa, S. Nakagawa and I. Kurohara, (1977): "Cyclic Undrained Triaxial Testing Using Undisturbed Sand Samples With Fine Content." Proc, 12th Annual Meeting Japanese Soc. Soil Mech. Found. Eng. p. 397—400. (In Japanese)
7) M. Fukuoka, K. Ishihara, Y. Yoshida, (1978): "Liquefaction Analysis of Sand Deposits." Special Research On Natural Calamities, Ministry of Education. No. a—52—3, p. 41—66. (In Japanese)
8) H. J. Gibbs, W. G. Holtz, (1957): "Research on Determining the Density of Sands by Spontaneous Penetration Tests." Proc. 4th ICSMFF, London, Vol. 1
9) G. G. Meyerhof, (1957): "Discussion of Gibbs and Holtz Paper." Proc. 4th ICSMFE, London. Vol. III
10) G. Castro, (1975): "Liquefaction and Cyclic Mobility of Saturated Sands." Journal of the Geotechnical Engineering Division, ASCE. Vol. 101, No. GT 6, p. 551—569

砂質土の繰り返し非排水三軸強度と土質定数の関係

横田耕一郎・今井常雄

概　要

(目的)

地震時に地盤内に発生するせん断応力や地盤の保持している繰り返し非排水せん断強度を調べたり，その両者を比較する手法は良く知られている。これらの値は，地盤の液状化評価をする際用いられる。これらの値を決める方法には多くのものがあるが，最も精度がよいとされているものは，発生せん断応力に対しては地震時の地盤の応答計算であり，地盤の繰り返し非排水強度に対しては室内繰り返し非排水三軸試験である。本報告の目的は，繰り返し非排水三軸強度（以下 Rl_{20} と呼ぶ）の評価をするための有用な実験公式を作成することにある。実験式における Rl_{20} は，他の土質力学的定数を基礎として表現される。筆者等の新しい実験公式は，非常に数多くの繰り返し非排水三軸試験のデータより得られたものであり，公式化するにあたっては，以下に示すような多重回帰理論を用いた。

$$Rl_{20}=\beta_0+\Sigma\beta_t\cdot X_t$$

ここに

β_0：切片　β_t：重回帰係数　X_t：土質定数

(要約)

実験には軸載荷型の繰り返し三軸試験装置が用いられた。図—1および図—2には，それぞれ装置の概略図とセルの詳細図を示す。実験に用いた不攪乱試料は，沖積層あるいは埋立の砂層から，サンドサンプリングにより採取されたものである。すべての試料は採取後凍結されている。表—1には，実験に用いた試料を示す。

図—3には，実験の代表的な波形記録の例を示す。波形記録は基本的にはつぎの3種類である。

a　繰り返し軸載荷
b　繰り返し軸変位
c　過剰間隙水圧

図—4は，Rl_{20} の定義を図示したものである。Rl_{20} は20回の正弦波軸加振を供試体に与えたとき，供試体の軸歪両振幅を5%に達しせしめるような応力比（繰り返し軸応力を初期有効拘束圧の2倍で除した値）として定義される。

筆者等は，当初，Rl_{20} を表わす土質定数としてつぎの量を考えた。

a　有効上載圧　$\sigma v'$

b 乾燥密度 γ_d
c 相対密度 D_r
d 平均粒径 D_{50}
e 10%粒径 D_{10}
f 細粒分含有率 FC
g 標準貫入試験の打撃回数 N

しかしながら，データの入手，評価の難しいものを除外し，最終的には，σ_i，N値，D_{50}およびFCのみを用いることにした。

試料数は総計142個であり，それぞれの深度につき1試料（1試料は3～4供試体）が採取された。

図—5～図—12に，Rl_{20}と各種の土質定数との関係を示す。いずれの図もよい関係を示していない。そこで，重回帰分析の手法を用いることにした。

図—13は重回帰分析に用いた各変数間の相関係数を示したものである。当然のことではあるが，FCとD_{50}との相関係数が大きいのが目立つ。これら2つの変数は重相関式において同時に考慮することのないようにした。

表—2には，以上の検討結果より考え得るすべての重回帰分析の組合せを示す。Rl_{20}を用いた重回帰分析はすべての組合せについて行なったが，一方，$\log Rl_{20}$を用いた重回帰分析は，統計学的に有意と考えられる3組のみについて行なった。（図—14の①～③および図—15参照）。

Rl_{20}，$\log Rl_{20}$に対する計算結果を，重相関関係および分散比の形にして，それぞれ図—14および図—15に示す。これらの計算結果より，最も重相関関係の高いものは，$\log Rl_{20}$と$\log \sigma v'$，N, FCを組合せた場合であることがわかる。その実験式を示せば，つぎのようである。

$$\log Rl_{20} = -0.785 + N \cdot \log 1.012 + 0.0868 \log FC - 0.441 \log \sigma v'$$

すなわち，Rl_{20}は

$$Rl_{20} = 0.164 \cdot (1.012)^N \cdot (FC)^{0.0868} \cdot \sigma v'^{-0.441}$$ 本文の式(3)

図—16には式(3)を用いて計算したRl_{20}（計算Rl_{20}）と実測したRl_{20}（実測Rl_{20}）の比較を示す。図には，既存データを用いた両者の比較をも示してある。両者の関係はかなり良いことがわかる。

図—17には，既存の実験式（本文の式(5)）を用いて求めた計算値Rl_{20}を使い，図—16と同様の整理をしたものを示す。この図では，一般的傾向は認められない。式(5)と式(3)の大きな違いは，両式のN値と$\sigma v'$に関する依存の程度である。今日までの多くの研究では，きれいな砂の場合，繰り返し非排水せん断強度はN値に大きく影響されるといわれている。この観点から考えると，N値と繰り返し非排水せん断強度の関係においては，(5)式の方が従来からの見解とよく一致するようである。しかしながら，サンドサンプリングと，繰り返し非排水三軸試験の組合せより評価される，繰り返し非排水せん断強度を決定するための実験式という観点からは，(3)式の方が優れているようである。

別の観点にたてば，式(3)は，繰り返し非排水せん断強度の評価に関して，現在用いられているシステムの精度に疑問を投げかけるものともいえる。この分野の今後のよりいっそうの研究が待たれる。